P. A. Martin
Department of Mathematical and Computer Sciences,
Colorado School of Mines,
Golden, CO 80401-1887
e-mail: pamartin@mines.edu

J. R. Berger
Division of Engineering,
Colorado School of Mines,
Golden, CO 80401-1887
e-mail: jberger@mines.edu

On Mechanical Waves Along Aluminum Conductor Steel Reinforced (ACSR) Power Lines

The propagation of elastic waves along composite wire rope is considered. The rope is modeled as co-axial layers of cylindrically anisotropic material. Simple kinematical assumptions lead to a "rod theory" for the wire rope, consisting of three coupled one-dimensional wave equations. Solutions of these equations are found. Results for a particular aluminum conductor steel reinforced (ACSR) conductor are described in detail. The slowest mode is found to be mainly torsional and mainly nondispersive in character. The other two modes are dispersive and have small torsional components.
[DOI: 10.1115/1.1491269]

1 Introduction

We are interested in the propagation of mechanical waves along overhead power lines. These are often composite structures known as aluminum conductor steel reinforced (ACSR) electrical conductors. These are composite wire ropes consisting of a central steel wire rope surrounded by several aluminum wires. Our interest stems from the potential use of mechanical waves to detect defects in ACSR power lines.

It is known that fatigue failure of strands in ACSR power lines is the most common form of damage, resulting from various forms of vibrations—aeolian, galloping, and wake-induced ([1]). Two regions of an ACSR power line can be distinguished: the region near the points of support and the region further away, "out in the span." Most fatigue damage seems to occur in the first region ([1] p. 51). In this region, the mechanical problem is very complicated and three-dimensional: one must take into account such features as interstrand slippage, suspension clamps and armor rods. Damage may also occur in the second region, sometimes induced by corrosion, and it is here that there is scope for some simpler models.

In a previous paper ([2]), we considered the propagation of torsional waves along a bimaterial elastic cylinder, composed of a steel circular cylindrical core surrounded by a co-axial aluminum cladding. The interface between the core and the cladding was assumed to be imperfect, so that some slipping was allowed. This model accounts well for the composite nature of an ACSR power line, and the imperfect-interface conditions include a parameter that may be varied. Moreover, it is possible that this model could be developed further, so as to treat the region near the points of support.

However, some features of the problem are not included, the most important of these being the anisotropy of wire rope. Thus: "The static response of axially loaded wire rope clearly points out the coupling between the axial and rotational displacements" ([3], p. 244). It follows that any plausible model of a wire rope should take this coupling into account. This paper is concerned with the development of such models for the dynamic response of wire rope.

The simplest models are based on a strength-of-materials approach, in which one writes

$$F = A_1\varepsilon + A_2\chi \quad \text{and} \quad M = A_3\varepsilon + A_4\chi, \tag{1}$$

where F is the axial force acting at an arbitrary cross section of the wire rope, M is the axial twisting moment, ε is the axial strain, χ is the rotation per unit length, and A_1, A_2, A_3, and A_4 are constants ([4]). This model has been used for the static response of ACSR cables by McConnell and Zemke [5], and it has been extended to include bending moments ([6,7]).

Equation (1) is a constitutive relation for the wire rope. Clearly, the coefficients A_i will depend on the details of the rope's construction. Much effort has been directed at obtaining analytical expressions for A_i; see, for example, [4,8], and references therein. For ACSR applications, see [4], Section 3.9 and [5]. One can also attempt to determine A_i experimentally ([9,5]). The diagonal coefficients A_1 (relating two axial quantities) and A_4 (relating two rotational quantities) may be obtained using standard test equipment, but the off-diagonal coefficients A_2 and A_3 require more specialized techniques. A third option is to adopt a hybrid scheme, whereby A_1 and A_4 are determined by analytical approximations or static experiments, but A_2 and A_3 are found using information obtained from dynamic experiments. This option will be mentioned in Section 2.

One question that arises is: does $A_2 = A_3$? Costello [4], Section 3.9, has calculated A_i for a particular ACSR cable, and found that $A_1 = 1.21\times10^6$ lb, $A_2 = 1.69\times10^4$ in lb, $A_3 = 1.61\times10^4$ in lb, and $A_4 = 5.55\times10^2$ in^2 lb, with $A_2/A_3 \simeq 1.05$. For a steel wire rope used in marine applications, Samras et al. [9] found experimentally that $A_1 = 4.44\times10^6$ lb, $A_2 = 2.23\times10^5$ in lb, $A_3 = 2.36\times10^5$ in lb, and $A_4 = 1.43\times10^4$ in^2 lb, with $A_2/A_3 \simeq 0.94$. Thus, it is reasonable to assume that $A_2 = A_3$. Moreover, this equality follows from the assumption that the wire rope is genuinely elastic; it seems to be a good approximation for real wire ropes, where constituent wires may slip, for example.

Following on from Eq. (1), one can write down equations of motion, in the form of two coupled wave equations for the axial displacement (w) and the angular rotation (ϕ),

$$A_1\frac{\partial^2 w}{\partial z^2} + A_2\frac{\partial^2 \phi}{\partial z^2} = m\frac{\partial^2 w}{\partial t^2}, \tag{2}$$

$$A_3\frac{\partial^2 w}{\partial z^2} + A_4\frac{\partial^2 \phi}{\partial z^2} = I\frac{\partial^2 \phi}{\partial t^2}, \tag{3}$$

where m is the mass per unit length and I is the mass moment of inertia per unit length about the central axis. (Further details and references are given in Section 2.) These equations permit wave motion, and this is investigated in Section 2. There are two wave speeds. In general, each torsional wave is accompanied by a longitudinal wave of the same shape but with a different amplitude.

Contributed by the Applied Mechanics Division of THE AMERICAN SOCIETY OF MECHANICAL ENGINEERS for publication in the ASME JOURNAL OF APPLIED MECHANICS. Manuscript received by the ASME Applied Mechanics Division, Sept. 6, 2001; final revision, Jan. 9, 2002. Associate Editor: A. K. Mal. Discussion on the paper should be addressed to the Editor, Prof. Robert M. McMeeking, Department of Mechanical and Environmental Engineering University of California–Santa Barbara, Santa Barbara, CA 93106-5070, and will be accepted until four months after final publication of the paper itself in the ASME JOURNAL OF APPLIED MECHANICS.

In Section 3, we develop an alternative theory, based on the exact stress equations of motion for a composite anisotropic elastic cylinder. The cylinder consists of co-axial layers, each of which is made of a cylindrically anisotropic elastic material. Simple kinematical assumptions are made, leading to a system of three coupled one-dimensional wave equations:

$$A_1\frac{\partial^2 w}{\partial z^2}+A_2\frac{\partial^2 \phi}{\partial z^2}+A_5\frac{\partial^2 u}{\partial z^2}+B_1\frac{\partial u}{\partial z}=m\frac{\partial^2 w}{\partial t^2}, \tag{4}$$

$$A_2\frac{\partial^2 w}{\partial z^2}+A_4\frac{\partial^2 \phi}{\partial z^2}+A_6\frac{\partial^2 u}{\partial z^2}+B_2\frac{\partial u}{\partial z}=I\frac{\partial^2 \phi}{\partial t^2}, \tag{5}$$

$$A_5\frac{\partial^2 w}{\partial z^2}+A_6\frac{\partial^2 \phi}{\partial z^2}+A_7\frac{\partial^2 u}{\partial z^2}-B_1\frac{\partial w}{\partial z}-B_2\frac{\partial \phi}{\partial z}-B_3 u=I\frac{\partial^2 u}{\partial t^2}. \tag{6}$$

Here, u gives the radial displacement. In general, this 3×3 system does not reduce to the 2×2 system, Eqs. (2) and (3), when $u=0$, which is an underlying assumption in the derivation of the 2×2 system. On the other hand, the 3×3 system does reduce to well known equations for the approximate description of waves in *isotropic* elastic rods ([10] Section 8.3).

Our model for the wire rope is called *semi-continuous* by Cardou and Jolicoeur [11] in their thorough review article: all the strands in each co-axial layer of the rope are ''homogenized'' into an elastic continuum. This idea was first used by Hobbs and Raoof [12]; they regarded each layer as a thin orthotropic sheet. It has been developed further by Cardou and his students ([13–15]). They do not regard the layers as thin, and they permit the orthotropy axes of the material of each layer to be aligned in directions that differ from the global cylindrical polar coordinate axes. We have extended this model to dynamic situations.

The coefficients occurring in Eqs. (4)–(6) are given in terms of certain integrals of the elastic stiffnesses of each layer over a typical cross section. Once these are known, wave propagation along the wire rope can be studied. For an example, we present some numerical results for a simple seven-wire ACSR conductor. Three distinct modes are found. The slowest mode is mainly torsional and mainly nondispersive in character. Such a mode could be excited by a device (transducer) designed to launch torsional waves. The two other modes are dispersive and have small torsional components.

2 The Samras-Skop-Milburn (SSM) Equations of Motion

Let z be distance along the wire rope and let t be the time. Let w be the axial displacement and let ϕ be the angular rotation. We use the constitutive relations (1), in which $\varepsilon=\partial w/\partial z$ and $\chi=\partial\phi/\partial z$, whence

$$F=A_1\frac{\partial w}{\partial z}+A_2\frac{\partial \phi}{\partial z} \quad \text{and} \quad M=A_3\frac{\partial w}{\partial z}+A_4\frac{\partial \phi}{\partial z}. \tag{7}$$

Then, a balance of forces and moments acting on an elementary slice of the wire rope gives Eqs. (2) and (3), which are approximate, one-dimensional equations of motion for the wire rope. They were derived by Samras, Skop, and Milburn [9]; we call Eqs. (2) and (3) the *SSM system*. This 2×2 system has been used in several subsequent papers, including [3,16–18].

It is of interest to obtain solutions to the SSM system. If we eliminate ϕ, say, we obtain a single fourth-order linear partial differential equation for w,

$$mI\frac{\partial^4 w}{\partial t^4}-(IA_1+mA_4)\frac{\partial^4 w}{\partial t^2\partial z^2}+(A_1A_4-A_2A_3)\frac{\partial^4 w}{\partial z^4}=0. \tag{8}$$

This has traveling-wave solutions of the form $w(z,t)=f(z-ct)$, where f is an arbitrary function (with four continuous derivatives) and there are four possible wavespeeds c, given by the roots of

$$mIc^4-c^2(IA_1+mA_4)+A_1A_4-A_2A_3=0; \tag{9}$$

these roots are given by

$$c^2=\{IA_1+mA_4\pm\sqrt{(IA_1-mA_4)^2+4mIA_2A_3}\}/(2mI). \tag{10}$$

We observe that these are the eigenvalues of the matrix

$$\mathbf{A}_2=\begin{pmatrix} A_1/m & A_2/m \\ A_3/I & A_4/I \end{pmatrix}.$$

Thus, we obtain two positive values of c and two negative values. The positive values correspond to different wavespeeds for waves propagating in the positive z direction; we will denote these by c_1 and c_2.

We can rewrite Eq. (9) as $A_2A_3=(mc^2-A_1)(Ic^2-A_4)$. If we assume that $A_2=A_3$ and we have good estimates for A_1 and A_4 (perhaps obtained from fairly standard static measurements on the wire rope), m and I, we could then calculate A_2 using a measurement of wavespeed c along the rope.

Returning to Eqs. (2) and (3), we could eliminate w instead of ϕ. This shows that ϕ satisfies exactly the same equation as w, namely Eq. (8), and so admits the same wavespeeds.

Next, let us look for solutions of Eqs. (2) and (3) in the form

$$w(z,t)=f(\xi) \quad \text{and} \quad \phi(z,t)=g(\xi), \tag{11}$$

where $\xi=z-ct$ and c solves Eq. (9). We obtain

$$\left.\begin{aligned}(A_1-mc^2)f''+A_2g''=0,\\ A_3f''+(A_4-Ic^2)g''=0,\end{aligned}\right\}$$

so that $(f'',g'')^T$ is an eigenvector of $\mathbf{A}_2$ corresponding to the eigenvalue c^2. Integrating twice, we see that

$$f(z-ct)=G(c)g(z-ct), \tag{12}$$

where the factor G is given by $G(c)=A_2/(mc^2-A_1)=(Ic^2-A_4)/A_3$. (When we integrated, we discarded terms of the form $C_1\xi+C_2$, where C_1 and C_2 are constants of integration. Such terms do satisfy Eqs. (2) and (3), as do any functions that are linear in both z and t, but they are not usually of interest.)

Equation (12) shows that if there is a torsional wave, ϕ, propagating at speed c, then it will be accompanied by an axial wave, w, propagating at the same speed and with the same shape, but with a different amplitude. For this conclusion to be valid, we require that there is actual coupling between axial and torsional motions; for a solid isotropic rod, we would have $A_2=A_3=0$, and then the axial and torsional waves can exist independently (as Eqs. (2) and (3) decouple).

This completes our study of the SSM system. In the next section, we attempt to give a more rational derivation of one-dimensional wave equations modeling the wire rope. We shall see that the SSM system should be replaced by a 3×3 system, in general.

3 An Approximate Theory for Waves in a Wire Rope

3.1 Stress Equations of Motion. In cylindrical polar coordinates (r,θ,z), the exact stress equations of motion are ([10], p. 600)

$$\frac{\partial}{\partial r}\tau_{rr}+\frac{1}{r}\frac{\partial}{\partial\theta}\tau_{r\theta}+\frac{\partial}{\partial z}\tau_{rz}+\frac{1}{r}(\tau_{rr}-\tau_{\theta\theta})=\rho\frac{\partial^2 u_r}{\partial t^2}, \tag{13}$$

$$\frac{\partial}{\partial r}\tau_{r\theta}+\frac{1}{r}\frac{\partial}{\partial\theta}\tau_{\theta\theta}+\frac{\partial}{\partial z}\tau_{\theta z}+\frac{2}{r}\tau_{r\theta}=\rho\frac{\partial^2 u_\theta}{\partial t^2}, \tag{14}$$

$$\frac{\partial}{\partial r}\tau_{rz}+\frac{1}{r}\frac{\partial}{\partial\theta}\tau_{\theta z}+\frac{\partial}{\partial z}\tau_{zz}+\frac{1}{r}\tau_{rz}=\rho\frac{\partial^2 u_z}{\partial t^2}, \tag{15}$$

where (u_r,u_θ,u_z) is the displacement, ρ is the mass density, and τ_{ij} are the stress components. We seek approximate solutions of these equations for a wire rope.

We model the wire rope as a circular cylinder of radius a. The cylinder consists of a cylindrical core, $0 \leq r < a_0$, and N co-axial layers, $a_{i-1} < r < a_i$, $i=1,2,\ldots,N$, with $a_N = a$. Thus, there are N interfaces, $r = a_{i-1}$, $i=1,2,\ldots,N$. The outer surface is free of tractions,

$$\tau_{rr} = \tau_{r\theta} = \tau_{rz} = 0 \quad \text{on} \quad r = a. \tag{16}$$

In general, the N interfaces may be imperfect: Slippage may occur. They could be modeled using one of several available models of imperfect interfaces; see [2] or [19].

In order to develop a ''rod theory'' for wire rope, we begin with some kinematical assumptions. Thus, we assume that

$$u_r = ru(z,t), \quad u_\theta = r\phi(z,t) \quad \text{and} \quad u_z = w(z,t), \tag{17}$$

where u, ϕ and w are to be found. Here, the approximations for u_r and u_z are usually made for longitudinal motions ([10], p. 511), whereas the approximation for u_θ means that cross sections can rotate about the central axis at $r=0$. One consequence of Eq. (17) is that the θ-derivative terms in Eqs. (13)–(15) are zero.

We are going to integrate Eqs. (13)–(15) across an arbitrary cross section $\mathcal{C}$ of the wire rope. We have

$$\int_0^a r\frac{\partial}{\partial r}\tau_{rz}dr = \sum_{i=0}^{N}\int_{a_{i-1}}^{a_i} r\frac{\partial}{\partial r}\tau_{rz}dr = \sum_{i=0}^{N}\left\{ [r\tau_{rz}]_{a_{i-1}}^{a_i} - \int_{a_{i-1}}^{a_i}\tau_{rz}dr\right\} = I_z - \int_0^a \tau_{rz}dr,$$

where $a_{-1}=0$, we have used Eq. (16),

$$I_z = \sum_{i=0}^{N-1} a_i[\tau_{rz}(a_i,z,t)]$$

and

$$[f(a_i,z,t)] = \lim_{r\to a_i^-} f(r,z,t) - \lim_{r\to a_i+} f(r,z,t)$$

gives the jump in a quantity f across an interface at $r=a_i$. Thus, integrating Eq. (15) across $\mathcal{C}$, we obtain

$$\frac{\partial}{\partial z}\int_{\mathcal{C}}\tau_{zz}dA + 2\pi I_z = m\frac{\partial^2 w}{\partial t^2} \tag{18}$$

where $dA = rdrd\theta$ and $m = \int_{\mathcal{C}}\rho dA$ is the mass per unit length of the wire rope.

We use a similar procedure with Eqs. (13) and (14), the difference being that we multiply both by r before integrating over $\mathcal{C}$. We obtain

$$\frac{\partial}{\partial z}\int_{\mathcal{C}} r\tau_{rz}dA - \int_{\mathcal{C}}(\tau_{rr}+\tau_{\theta\theta})dA + 2\pi I_r = I\frac{\partial^2 u}{\partial t^2} \tag{19}$$

and

$$\frac{\partial}{\partial z}\int_{\mathcal{C}} r\tau_{\theta z}dA + 2\pi I_\theta = I\frac{\partial^2 \phi}{\partial t^2}, \tag{20}$$

where

$$I_r = \sum_{i=0}^{N-1} a_i^2[\tau_{rr}(a_i,z,t)], \quad I_\theta = \sum_{i=0}^{N-1} a_i^2[\tau_{r\theta}(a_i,z,t)]$$

and $I = \int_{\mathcal{C}}\rho r^2 dA$ is the mass moment of inertia per unit length about the central axis.

Note that if the wire rope was a solid circular cylinder of radius a, with constant density and welded interfaces, then we would have $I_r = I_\theta = I_z = 0$, $I = (1/2)ma^2$ and $m = \pi\rho a^2$.

The quantities I_r, I_θ, and I_z give the total contributions from the possible discontinuities in the traction across each of the N interfaces. We assume that

$$I_r = I_\theta = I_z = 0. \tag{21}$$

This simplifies the analysis, of course, but it also turns out to be realistic ([1], p. 54):

> Real conductors do not have frictionless strands, and, for the small amounts of flexure experienced due to vibration waves out in the span, the friction present between strands is normally great enough to prevent gross sliding between them. The relative axial movements of the strands are absorbed in largely elastic shear strains around the small areas of interstrand contact. The amounts of movement are not great enough to build up tractions that exceed the threshold of sliding.

On the other hand, the assumption (21) cannot be justified near the points of support.

3.2 Cylindrically Anisotropic Materials. Next, we need constitutive relations for the materials of the wire rope. We assume that each layer is composed of a cylindrically anisotropic elastic solid. Letting $(r,\theta,z)=(1,2,3)$, Hooke's law becomes

$$\tau_{ij} = C_{ijkl}\varepsilon_{kl}, \tag{22}$$

where ε_{ij} are the strain components, and we emphasize that the stiffnesses C_{ijkl} are referred to cylindrical polar coordinates; see [20] and [21] for more details. We assume further that each layer of the wire is homogeneous, so that the stiffnesses are constant within each layer. Thus, $C_{ijkl} = C_{ijkl}(r)$ are piecewise-constant functions of r.

The strains are given as follows ([20], p. 2399):

$$\varepsilon_{rr} = \frac{\partial u_r}{\partial r} = u, \quad \varepsilon_{\theta\theta} = \frac{1}{r}\frac{\partial u_\theta}{\partial\theta} + \frac{u_r}{r} = u,$$

$$\varepsilon_{zz} = \frac{\partial u_z}{\partial z} = \frac{\partial w}{\partial z}, \quad \varepsilon_{r\theta} = \frac{1}{2}\left(\frac{1}{r}\frac{\partial u_r}{\partial\theta} + \frac{\partial u_\theta}{\partial r} - \frac{u_\theta}{r}\right) = 0,$$

$$\varepsilon_{rz} = \frac{1}{2}\left(\frac{\partial u_z}{\partial r} + \frac{\partial u_r}{\partial z}\right) = \frac{1}{2}r\frac{\partial u}{\partial z},$$

$$\varepsilon_{\theta z} = \frac{1}{2}\left(\frac{\partial u_\theta}{\partial z} + \frac{1}{r}\frac{\partial u_z}{\partial\theta}\right) = \frac{1}{2}r\frac{\partial\phi}{\partial z}.$$

The corresponding stresses are given by Eq. (22) as

$$\tau_{ij} = C_{ij11}\varepsilon_{rr} + C_{ij22}\varepsilon_{\theta\theta} + C_{ij33}\varepsilon_{zz} + 2C_{ij12}\varepsilon_{r\theta} + 2C_{ij23}\varepsilon_{\theta z} + 2C_{ij13}\varepsilon_{rz} = (C_{ij11}+C_{ij22})u + C_{ij33}\frac{\partial w}{\partial z} + C_{ij23}r\frac{\partial\phi}{\partial z} + C_{ij13}r\frac{\partial u}{\partial z}.$$

Thus

$$\tau_{rz} = \tau_{13} = (C_{15}+C_{25})u + C_{35}\frac{\partial w}{\partial z} + C_{45}r\frac{\partial\phi}{\partial z} + C_{55}r\frac{\partial u}{\partial z},$$

$$\tau_{\theta z} = \tau_{23} = (C_{14}+C_{24})u + C_{34}\frac{\partial w}{\partial z} + C_{44}r\frac{\partial\phi}{\partial z} + C_{45}r\frac{\partial u}{\partial z},$$

$$\tau_{r\theta} = \tau_{12} = (C_{16}+C_{26})u + C_{36}\frac{\partial w}{\partial z} + C_{46}r\frac{\partial\phi}{\partial z} + C_{56}r\frac{\partial u}{\partial z},$$

$$\tau_{zz} = \tau_{33} = (C_{13}+C_{23})u + C_{33}\frac{\partial w}{\partial z} + C_{34}r\frac{\partial\phi}{\partial z} + C_{35}r\frac{\partial u}{\partial z},$$

$$\tau_{rr} = \tau_{11} = (C_{11}+C_{12})u + C_{13}\frac{\partial w}{\partial z} + C_{14}r\frac{\partial\phi}{\partial z} + C_{15}r\frac{\partial u}{\partial z},$$

$$\tau_{\theta\theta} = \tau_{22} = (C_{12}+C_{22})u + C_{23}\frac{\partial w}{\partial z} + C_{24}r\frac{\partial\phi}{\partial z} + C_{25}r\frac{\partial u}{\partial z},$$

where we have used the usual contracted notation $C_{\alpha\beta}$ for C_{ijkl} ([22], Section 2.3). Note that these expressions make use of 20 of the 21 stiffnesses, the exception being C_{66}.

3.3 One-Dimensional Equations of Motion. We use the expressions above for τ_{ij} in Eqs. (18), (19), and (20), together with Eq. (21), and obtain Eqs. (4)–(6), wherein

$$A_1=\int_{\mathcal{C}} C_{33}dA, \quad A_2=\int_{\mathcal{C}} rC_{34}dA, \quad A_4=\int_{\mathcal{C}} r^2C_{44}dA,$$

$$A_5=\int_{\mathcal{C}} rC_{35}dA, \quad A_6=\int_{\mathcal{C}} r^2C_{45}dA, \quad A_7=\int_{\mathcal{C}} r^2C_{55}dA,$$

$$B_1=\int_{\mathcal{C}} (C_{13}+C_{23})dA, \quad B_2=\int_{\mathcal{C}} r(C_{14}+C_{24})dA,$$

$$B_3=\int_{\mathcal{C}} (C_{11}+C_{22}+2C_{12})dA.$$

Note that these expressions make use of 13 different elastic stiffnesses.

Equations (4)–(6) are three coupled one-dimensional wave equations for u, ϕ, and w, defined by Eq. (17). This 3×3 system should be compared with the 2×2 SSM system (which was derived by strength-of-materials arguments). We do this next.

3.4 Comparison With the Samras-Skop-Milburn (SSM) System. We see immediately that Eqs. (4) and (5) reduce to Eqs. (2) and (3), respectively, if $u\equiv0$ (no radial displacement). Then, the third equation, Eq. (6), becomes

$$A_5\frac{\partial^2 w}{\partial z^2}+A_6\frac{\partial^2 \phi}{\partial z^2}-B_1\frac{\partial w}{\partial z}-B_2\frac{\partial \phi}{\partial z}=0. \tag{23}$$

Now, we know that the SSM system has traveling-wave solutions, given by Eqs. (11) and (12). When these are substituted in Eq. (23), we obtain an ordinary differential equation for $g(\xi)$, with solution $g(\xi)=e^{\gamma\xi}$ where $\gamma=(B_1G+B_2)/(A_5G+A_6)$, provided A_5 and A_6 are not both zero. This particular exponential solution is not of interest to us, as we want to consider the propagation of bounded pulses along the wire rope; therefore, we discard this solution. If $A_5=A_6=0$ (this case will arise in Section 4.1), Eq. (23) reduces to $B_1G+B_2=0$. This may be satisfied for one value of c^2 given by Eq. (10), but not both.

Another way to satisfy Eq. (23) identically is to require that the stiffnesses are such that

$$A_5=A_6=B_1=B_2=0. \tag{24}$$

These conditions involve the stiffnesses and radius of each concentric layer of the composite cylinder. They will be satisfied if the material in each layer satisfies $C_{35}=C_{45}=0$, $C_{13}=-C_{23}$ and $C_{14}=-C_{24}$.

We conclude that, in very special circumstances, our 3×3 system reduces to the SSM system, together with $u\equiv0$.

Let us also calculate the forces and moments acting on a cross section $\mathcal{C}$ of the wire rope. The axial force is given by

$$F=\int_{\mathcal{C}} \tau_{zz}dA=A_1\frac{\partial w}{\partial z}+A_2\frac{\partial \phi}{\partial z}+A_5\frac{\partial u}{\partial z}+B_1u \tag{25}$$

and the axial twisting moment is given by

$$M=\int_{\mathcal{C}} r\tau_{\theta z}dA=A_2\frac{\partial w}{\partial z}+A_4\frac{\partial \phi}{\partial z}+A_6\frac{\partial u}{\partial z}+B_2u.$$

Both of these reduce to Eq. (7), provided $u\equiv0$ *or* Eq. (24) holds.

3.5 Waves. Before looking for solutions of Eqs. (4)–(6), it is convenient to introduce dimensionless variables. Let c_0 be a typical wave speed for elastic waves in the rope. For a length scale, we shall use a, the outer radius of the rope's cross section. (Phillips and Costello [17] use the length of the rope.) Define

$$z'=\frac{z}{a}, \quad t'=\frac{c_0t}{a}, \quad u'=u\sqrt{\frac{I}{ma^2}},$$

$$\phi'=\phi\sqrt{\frac{I}{ma^2}} \text{ and } w'=\frac{w}{a}, \tag{26}$$

where the primes signify dimensionless quantities. Then, Eqs. (4)–(6) become

$$A_1'\frac{\partial^2 w'}{\partial z'^2}+A_2'\frac{\partial^2 \phi'}{\partial z'^2}+A_5'\frac{\partial^2 u'}{\partial z'^2}+B_1'\frac{\partial u'}{\partial z'}=\frac{\partial^2 w'}{\partial t'^2}, \tag{27}$$

$$A_2'\frac{\partial^2 w'}{\partial z'^2}+A_4'\frac{\partial^2 \phi'}{\partial z'^2}+A_6'\frac{\partial^2 u'}{\partial z'^2}+B_2'\frac{\partial u'}{\partial z'}=\frac{\partial^2 \phi'}{\partial t'^2}, \tag{28}$$

$$A_5'\frac{\partial^2 w'}{\partial z'^2}+A_6'\frac{\partial^2 \phi'}{\partial z'^2}+A_7'\frac{\partial^2 u'}{\partial z'^2}-B_1'\frac{\partial w'}{\partial z'}-B_2'\frac{\partial \phi'}{\partial z'}-B_3'u'=\frac{\partial^2 u'}{\partial t'^2}, \tag{29}$$

where

$$A_1'=\frac{A_1}{mc_0^2}, \quad A_2'=\frac{A_2}{c_0^2\sqrt{mI}}, \quad A_4'=\frac{A_4}{c_0^2I}, \quad A_5'=\frac{A_5}{c_0^2\sqrt{mI}},$$

$$A_6'=\frac{A_6}{c_0^2I}, \quad A_7'=\frac{A_7}{c_0^2I}, \quad B_1'=\frac{aB_1}{c_0^2\sqrt{mI}}, \quad B_2'=\frac{aB_2}{c_0^2I},$$

$$\text{and } B_3'=\frac{a^2B_3}{c_0^2I}.$$

Henceforth, we drop all the primes.

The scaling introduced above may seem complicated but it has *three* beneficial consequences. First, all equations and coefficients are *dimensionless*. Second, it will lead to a *Hermitian* coefficient matrix when we seek solutions proportional to $\exp\{ik(z-\alpha t)\}$ (see Eq. (32) below) and, third, the wave speed α will be determined by solving an eigenvalue problem (rather than a *generalized* eigenvalue problem).

Thus, we seek solutions in the form

$$u=u_0e^{ik\xi}, \quad \phi=\phi_0e^{ik\xi} \text{ and } w=w_0e^{ik\xi}, \tag{30}$$

where $\xi=z-\alpha t$, u_0, ϕ_0, and w_0 are constants, k is a nonzero dimensionless real wave number, and α is a dimensionless wave speed; the actual wave speed is αc_0 and the actual wavelength is $2\pi a/k$. Substituting Eq. (30) in Eqs. (27)–(29) gives

$$(\mathbf{A}-\alpha^2\mathbf{I})\mathbf{x}=\mathbf{0}, \tag{31}$$

where

$$\mathbf{A}=\begin{pmatrix} A_1 & A_2 & A_5-iB_1/k \\ A_2 & A_4 & A_6-iB_2/k \\ A_5+iB_1/k & A_6+iB_2/k & A_7+B_3/k^2 \end{pmatrix} \tag{32}$$

and $\mathbf{x}^T=(w_0,\phi_0,u_0)$. Equation (31) will have a nontrivial solution provided that

$$\det(\mathbf{A}-\alpha^2\mathbf{I})=0, \tag{33}$$

which is a cubic in α^2. The three solutions for α^2 are all real. This follows by noting that $\mathbf{A}$ is a complex Hermitian matrix so that $\bar{\mathbf{x}}^T\mathbf{A}\mathbf{x}$ is real (where the overbar denotes complex conjugation).

We would like to know that the real solutions for α^2 are *all positive*, so that we have six real solutions for α. With $\lambda=\alpha^2$, we can write Eq. (33) as

$$f(\lambda)\equiv\lambda^3+d_2\lambda^2+d_1\lambda+d_0=0, \tag{34}$$

where the coefficients d_i are known in terms of the entries of $\mathbf{A}$. We know that $f(\lambda)=0$ has real roots only, so elementary consid-

erations (such as sketching the graph of $f(\lambda)$) will lead to conditions on d_i that are sufficient to guarantee that all the roots are positive. For example, we must have $f(0)<0$, which yields $\det(\mathbf{A})>0$. We must also have two positive turning points, and this yields $d_2<0$.

Let us make three further remarks. First, despite the appearance of first derivatives with respect to z, the system (27)–(29) is symmetric in z. In other words, if there is a solution proportional to e^{ikz}, then there is another proportional to e^{-ikz}, with the same value of α. For $\det(\bar{\mathbf{A}}-\alpha^2\mathbf{I})=\det(\mathbf{A}-\alpha^2\mathbf{I})$, as $\mathbf{A}$ is Hermitian. Second, as $\mathbf{A}$ depends on k, so too does α: the waves are *dispersive*, unlike the solutions of the SSM system. Third, having found the eigenvalues α^2, the relative displacement amplitudes are given by the corresponding eigenvector $\mathbf{x}=(w_0,\phi_0,u_0)^T$ of $\mathbf{A}$.

4 Cylindrically Orthotropic Materials

The theory developed in Section 3 is fairly general. As a special case, we can suppose that the material of each layer is cylindrically orthotropic. For such materials, there are nine nontrivial stiffnesses, namely C_{11}, C_{12}, C_{13}, C_{22}, C_{23}, C_{33}, C_{44}, C_{55}, and C_{66}. It follows that $A_2=A_5=A_6=B_2=0$, so that the torsional component ϕ decouples from u and w. Equation (28) reduces to $A_4\partial^2\phi/\partial z^2=\partial^2\phi/\partial t^2$, the one-dimensional wave equation with wavespeed $\sqrt{A_4}$. Equations (27) and (29) reduce to

$$A_1\frac{\partial^2 w}{\partial z^2}+B_1\frac{\partial u}{\partial z}=\frac{\partial^2 w}{\partial t^2}, \tag{35}$$

$$A_7\frac{\partial^2 u}{\partial z^2}-B_1\frac{\partial w}{\partial z}-B_3 u=\frac{\partial^2 u}{\partial t^2}. \tag{36}$$

These can be solved, using Eq. (30). However, we do not pursue this here, as we are interested mainly in situations where the torsional motions do *not* decouple.

We remark that for *isotropic* materials, we can show that Eqs. (35) and (36) reduce to Eq. (8.3.148) in [10].

4.1 Rotated Coordinate Systems. Above, we considered a material with cylindrical orthotropy, where the principal axes are aligned with the cylindrical-polar coordinate axes. We saw that torsional motions decoupled from axial and radial motions.

Suppose, now, that the material of each layer is cylindrically orthotropic with respect to a different coordinate system, (r',θ',z'), with nine nontrivial elastic stiffnesses $C'_{\alpha\beta}$ ([14,15]). We want to express $C_{\alpha\beta}$ in terms of $C'_{\alpha\beta}$. (This is a standard calculation in tensor analysis.) Specifically, at a typical point P, the cylinder has three coordinate directions, namely, $1\equiv r$, $2\equiv\theta$ and $3\equiv z$. At the same point, the material has three principal directions, namely, $1'\equiv r'$, $2'\equiv\theta'$, and $3'\equiv z'$. We suppose that the r and r' directions coincide (at P), and that the (θ,z) directions are obtained by rotating the (θ',z') directions by an angle β about the r-direction. The stiffnesses transform according to

$$C_{ijkl}(\beta)=\Omega_{ip}\Omega_{jq}\Omega_{kr}\Omega_{ls}C'_{pqrs},$$

where

$$\Omega_{ij}(\beta)=\begin{pmatrix}1&0&0\\0&\cos\beta&\sin\beta\\0&-\sin\beta&\cos\beta\end{pmatrix}.$$

Explicit calculations show that the (symmetric) stiffness matrix referred to coordinates (r',θ',z'), which has the structure

$$\mathbf{C}'=\begin{pmatrix}C'_{11}&C'_{12}&C'_{13}&0&0&0\\&C'_{22}&C'_{23}&0&0&0\\&&C'_{33}&0&0&0\\&&&C'_{44}&0&0\\&&&&C'_{55}&0\\&&&&&C'_{66}\end{pmatrix},$$

is transformed into a (symmetric) stiffness matrix referred to coordinates (r,θ,z) with the structure

$$\mathbf{C}=\begin{pmatrix}C_{11}&C_{12}&C_{13}&C_{14}&0&0\\&C_{22}&C_{23}&C_{24}&0&0\\&&C_{33}&C_{34}&0&0\\&&&C_{44}&0&0\\&&&&C_{55}&C_{56}\\&&&&&C_{66}\end{pmatrix}. \tag{37}$$

Explicit expressions for $C_{\alpha\gamma}$ in terms of $C'_{\alpha\gamma}$ are given in Appendix A. A consequence of this structure of $\mathbf{C}$ is that $A_5=A_6=0$, leading to a slight simplification of the analysis in Section 3.

4.2 Transverse Isotropy. Transverse isotropy is a special case of cylindrical orthotropy. For such materials, there are five nontrivial stiffnesses; the (unrotated) stiffness matrix can be written as

$$\mathbf{C}'=\begin{pmatrix}C'_{11}&C'_{12}&C'_{13}&0&0&0\\&C'_{11}&C'_{13}&0&0&0\\&&C'_{33}&0&0&0\\&&&C'_{44}&0&0\\&&&&C'_{44}&0\\&&&&&\frac{1}{2}(C'_{11}-C'_{12})\end{pmatrix}.$$

In order to use the results in [14,15], it is convenient to introduce engineering constants. These are the longitudinal Young's modulus E_L, the transverse Young's modulus E_T, the longitudinal Poisson's ratio ν_L, the transverse Poisson's ratio ν_T, and the longitudinal shear modulus G_L. Then, using [15] (Eq. (2)) and [23] (Eqs. (2.25) and (2.36)), we obtain

$$C'_{11}=\frac{1-\gamma\nu_L^2}{\Delta}E_T,\quad C'_{12}=\frac{\nu_T+\gamma\nu_L^2}{\Delta}E_T,$$

$$C'_{13}=\frac{\nu_L(1+\nu_T)}{\Delta}E_L,\quad C'_{33}=\frac{1-\nu_T^2}{\Delta}E_L$$

and $C'_{44}=G_L$; here, $\gamma=E_L/E_T$ and $\Delta=1-\nu_T^2-2\gamma\nu_L^2(1+\nu_T)$. Note that $C'_{66}=(1/2)E_T/(1+\nu_T)$. After rotation, one obtains a matrix $\mathbf{C}$ with the same structure as Eq. (37).

For an isotropic material, $E_L=E_T=E$, $\nu_L=\nu_T=\nu$ and $G_L=\mu=(1/2)E/(1+\nu)$.

Following Jolicoeur and Cardou [14,15], we shall use this constitutive model (rotated transverse isotropy) for a composite wire rope. A specific example of a simple ACSR electrical conductor is considered in the next section.

5 A Simple Example of an Aluminum Conductor Steel Reinforced (ACSR) Conductor

In order to use the foregoing theory, we have to specify the physical characteristics of the wire rope and we have to estimate the elastic constants. Methods for doing this have been described by Jolicoeur and Cardou [14,15] in their analysis of the static

loading of wire rope. We follow their method closely, making use of some calculations of Costello ([4], Section 3.9). Thus, we consider a very simple ACSR conductor, consisting of six aluminum wires helically wound around a single straight steel-wire core. The steel wire has radius $r_s=1.70$ mm (0.067 in.). All the aluminum wires have radius $r_a=1.68$ mm (0.066 in.). In terms of the model described in Section 3, we have $N=1$, $a_0=r_s$ and $a_1=a=r_s+2r_a$. The aluminum wires have a helical radius of $h=r_s+r_a$ and a helical angle of $\beta=10$ deg. (These parameters are approximately those of the so-called Raven 6/1 ACSR conductor; see [24], Table 1–6).

Mass per Unit Length. Taking a cross section of the wire rope, we see that each aluminum wire has an approximately elliptical cross section, with a semi-minor axis of length r_a and a semi-major axis of length $r_a \sec\beta$; see [4], Fig. 3.1. Thus, each wire has a mass per unit length of $\pi\rho_a r_a^2 \sec\beta=m_a$, say, where ρ_a is the density of aluminum. Hence, if ρ_s is the density of steel,

$$\frac{m}{\pi\rho_a a^2}=\frac{\rho_s}{\rho_a}\left(\frac{r_s}{a}\right)+6\left(\frac{r_a}{a}\right)^2\sec\beta=0.998, \tag{38}$$

where we have used $\rho_s=7800$ kg/m^3 and $\rho_a=2700$ kg/m^3. Note that the mass of the wire rope is almost the same as that of a solid aluminum cylinder of the same diameter. Note also that our calculated value for m is consistent with the tabulated value of 216 kg/km for the Raven ACSR conductor; see [24], Table 1–6.

Moment of Inertia. The moment of inertia of an ellipse about an axis through its center (and perpendicular to its plane) is $(1/4)M(a^2+b^2)$, where M is its mass and a and b are the lengths of the semi-major and semi-minor axes. Then, using the parallel-axes theorem, we obtain

$$I=\frac{1}{2}\pi\rho_s r_s^4+6\left\{m_a h^2+\frac{1}{4}m_a r_a^2(1+\sec^2\beta)\right\}.$$

Hence, $I=0.357ma^2$; about 95% of this comes from the aluminum wires. (For comparison, a solid composite cylinder composed of a steel core of radius a_0 surrounded by an aluminum cladding of outer radius a has $I=0.422ma^2$.)

Stiffnesses. The steel core is isotropic with Young's modulus E_s and Poisson's ratio $\nu_s=0.25$. Thus $E_L=E_T=E_s$, $\nu_L=\nu_T=\nu_s$ and $G_L=0.4E_s$. The corresponding stiffnesses are $C_{11}=C_{33}=1.2E_s$ and $C_{12}=C_{13}=C_{44}=C_{66}=0.4E_s$.

Let aluminum have Young's modulus E_a and Poisson's ratio $\nu_a=0.33$. Then, from Eqs. (3), (9), and (12)–(14) in [15], the aluminum wires may be modeled using

$$\frac{E_L}{E_a}=\frac{3}{2}\frac{r_a}{h}\sec\beta=0.756,$$

$$\frac{\nu_L}{\nu_a}=\frac{E_T}{E_L}=\frac{1}{\gamma},\quad \frac{\nu_T}{\nu_a}=\frac{E_T}{E_a},$$

$$\frac{G_L}{E_a}=\frac{r_a^2(E_L/E_a)}{2(1+\nu_a)(r_a^2+h^2)(1+\cos^2\beta)}=0.0285$$

and

$$\frac{1}{E_T}=\frac{C_E}{\pi}\left\{\log\frac{\pi(r_s+r_a)}{X_c C_E}-\frac{1}{3}\right\},$$

where X_c is the contact force per unit length and, from [25], Table 33,

$$C_E=\frac{1-\nu_s^2}{E_s}+\frac{1-\nu_a^2}{E_a}=\frac{1.204}{E_a},$$

using $E_s=3E_a$. The calculation of X_c is described in Appendix B, using the method of Costello [4]. From Eq. (*B*6), we obtain

$$\pi(r_s+r_a)/(X_c C_E)=790.4h^2E_a/F,$$

where F is the (static) axial force on the wire rope. As an example, let us take $F=5000$ N (1124 lb). We take $E_a=7\times10^{10}$ N/m^2 whence $E_T=0.229E_a$. (Evidently, E_T will increase if F is increased, but the increase is not linear; in fact, E_T depends logarithmically on F, so that large changes in F will induce moderate changes in E_T.) Hence $\nu_T=0.08$, $\nu_L=0.10$, $\gamma=3.3$, and $\Delta=0.92$. Then, from Section 4.2, we obtain $C'_{11}=0.241E_a$, $C'_{12}=0.028E_a$, $C'_{13}=0.089E_a$, $C'_{33}=0.816E_a$, $C'_{44}=0.029E_a$ and $C'_{66}=0.106E_a$. Finally, the rotated stiffnesses are given by

$$\mathbf{C}=E_a\begin{pmatrix} 0.24 & 0.03 & 0.09 & 0.01 & 0 & 0 \\ & 0.23 & 0.11 & 0.01 & 0 & 0 \\ & & 0.78 & 0.11 & 0 & 0 \\ & & & 0.05 & 0 & 0 \\ & & & & 0.03 & -0.01 \\ & & & & & 0.10 \end{pmatrix},$$

using the relations given in Appendix A.

Averaged Stiffnesses. The coefficients A_1, A_2, A_4, A_5, A_6, A_7, B_1, B_2, and B_3 are defined in Section 3.3 by certain integrals of the stiffnesses over a cross section of the wire rope. Dimensionless versions of these coefficients are defined in Section 3.5, making use of m, I and a typical wave speed c_0, which we shall take to be the speed of shear waves in aluminum: $c_0^{-2}=2\rho_a(1+\nu_a)/E_a$. Thus, $mc_0^2=0.375\pi E_a a^2$, using $\nu_a=0.33$ and Eq. (38). Then

$$A_1=\frac{1}{mc_0^2}\int_{\mathcal{C}}C_{33}dA=\frac{\pi E_a a^2}{mc_0^2}\left\{\left(\frac{r_s}{a}\right)^2\frac{E_s}{E_a}\frac{C_{33}^s}{E_s}+\left[1-\left(\frac{r_s}{a}\right)^2\right]\frac{C_{33}^a}{E_a}\right\},$$

where the superscripts on C_{33} denote steel or aluminum, as appropriate. We have $r_s/a=0.337$, $E_s/E_a=3$, $C_{33}^s/E_s=1.2$ and $C_{33}^a/E_a=0.78$ whence $A_1=2.94$. The other coefficients are obtained similarly. Thus, we find that

$$A_1=2.94,\quad A_2=0.32,\quad A_4=0.24,\quad A_5=A_6=0,$$

$$A_7=0.17,\quad B_1=2.00,\quad B_2=0.096\quad\text{and}\quad B_3=11.61.$$

Waves. Having specified the mechanical properties of the ACSR conductor, we can now calculate the allowable wave modes, according to the theory described in Section 3.5. For a given dimensionless wave number k, the dimensionless wavespeeds α are given by solving Eq. (33), which can be written as a cubic in $\lambda=\alpha^2$, namely Eq. (34), in which

$$d_2=-(3.35+11.61k^{-2}),\quad d_1=1.14+32.91k^{-2}\quad\text{and}$$

$$d_0=-(0.103+6.14k^{-2}).$$

As d_0 and d_2 are both negative, for all k^2, the cubic has only positive real roots, so that all the wave speeds are real.

Numerical Results. We have solved Eq. (34) for α^2. In Fig. 1, we have plotted the three positive values of α, as a function of k. Evidently, we can denote these three values by $\alpha_i(k)$, $i=1, 2, 3$, with $0<\alpha_1<\alpha_2<\alpha_3$. We see that $\alpha_i(k)$ is a decreasing function of k. In fact, the lowest wave speed, α_1, is almost independent of k: for example, $\alpha_1(1)\simeq0.448$ and $\alpha_1(10)\simeq0.447$. Thus, the wave corresponding to α_1 is almost nondispersive: it travels with a speed of approximately $0.45c_0$, where c_0 is the speed of shear waves in aluminum.

Figure 1 also suggests that $\alpha_2(k)-\alpha_1(k)\to0$ as $k\to\infty$. This is false. To see this, let $k\to\infty$ in $\mathbf{A}$, and put $A_5=A_6=0$. Then, using the notation of Abramowitz and Stegun [26], Section 3.8.2, we calculate q^3+r^2, where $q=(1/3)d_1-(1/9)d_2^2$ and $r=(1/6)(d_1d_2-3d_0)-(1/27)d_2^3$. We find that

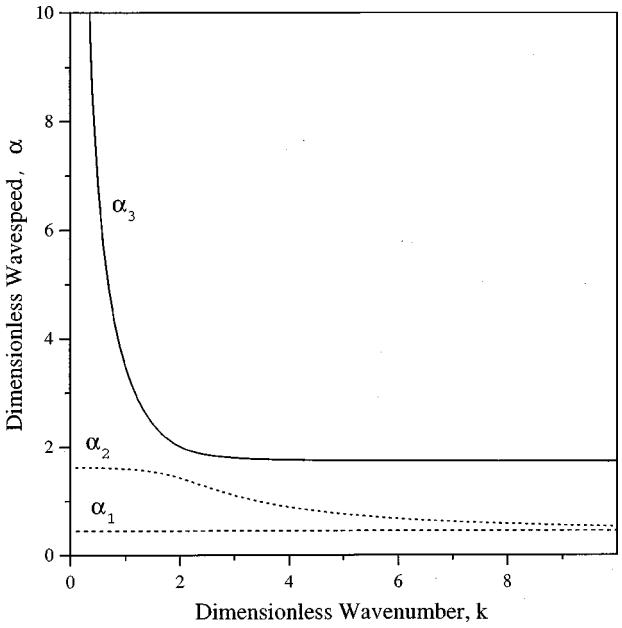

Fig. 1 The dimensionless wave speeds α_i as functions of dimensionless wave number k

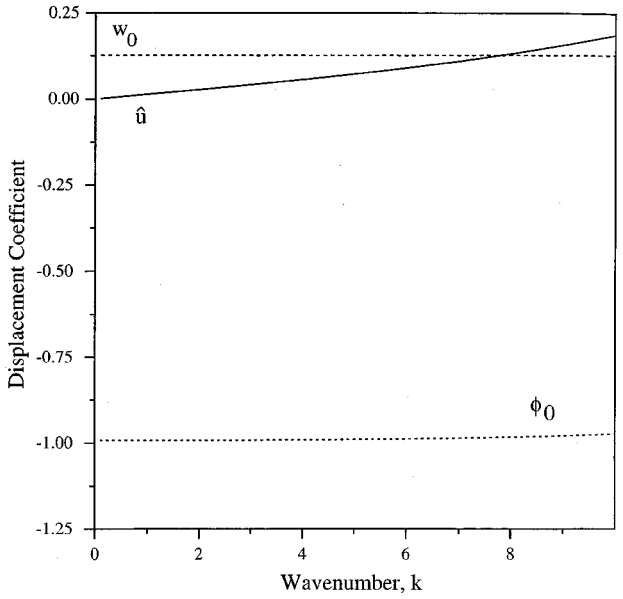

Fig. 2 The components of the dimensionless eigenvector $\mathbf{x}_1 = (w_0, \phi_0, i\hat{u})$ corresponding to the dimensionless wave speed α_1, as functions of dimensionless wave number k. This is the quasi-torsional mode.

$$q^3 + r^2 = -\frac{1}{108}\{(A_1 - A_4)^2 + 4A_2^2\}\{A_2^2 + (A_1 - A_7)(A_7 - A_4)\}^2,$$

which is negative, confirming that all the roots are real (when $k = \infty$). However, for our particular values of A_i, we obtain $q^3 + r^2 \simeq -0.02$, which is small, and so α_1 and α_2 will differ by a small but finite amount for large k. In fact, we find $\alpha_2(10) \simeq 0.523$ and $\alpha_3(10) \simeq 1.73$.

Next, we have calculated the eigenvectors $\mathbf{x}_i$ of $\mathbf{A}$, corresponding to α_i, where $\mathbf{x} = (w_0, \phi_0, u_0)^T$. We can arrange that $|\mathbf{x}| = 1$ and, as $A_5 = A_6 = 0$, it follows from Eq. (31) that we can take w_0 and ϕ_0 to be real and u_0 to be pure imaginary, $u_0 = i\hat{u}$, say. Then, taking the real part of Eq. (30), we obtain

$$u = -\hat{u}\sin k\xi, \quad \phi = \phi_0 \cos k\xi \quad \text{and} \quad w = w_0 \cos k\xi,$$

where $\xi = z - \alpha t$. Thus, the radial component is out of phase with the axial and torsional components. Then, the normalized eigenvectors show the physical character of each mode.

The three components of $\mathbf{x}_1$, corresponding to the lowest wavespeed α_1, are shown in Fig. 2, as a function of k. We see that this mode is a quasi-torsional mode: The axial and radial components are small. This weakly dispersive mode is the most important in the context of our application to ACSR conductors, because our transducers are designed to launch torsional waves.

The components of the eigenvector $\mathbf{x}_2$, corresponding to the wave speed α_2, are shown in Fig. 3, whereas $\mathbf{x}_3$ is shown in Fig. 4. We see that both of these modes have small torsional components. For $\mathbf{x}_2$, the axial component decreases with k and the radial component dominates, whereas the opposite situation occurs with $\mathbf{x}_3$.

6 Conclusions

In this paper, we have attempted to give a rational model for the propagation of elastic waves along composite wire ropes. The goal was to obtain one-dimensional differential equations of wave-equation type, with coefficients obtained from certain integrals over the cross section of the wire rope. Such equations are well known for waves in isotropic rods. We used simple kinematical assumptions, Eq. (17), but it is clear that various expansions in r could be used; see Boström [27] for a recent discussion of such methods.

We derived a set of three coupled partial differential equations, Eqs. (4)–(6). The coefficients in these equations are given as integrals involving the elastic stiffnesses of each layer of the composite wire rope, when regarded as a solid with cylindrical anisotropy. A basic difficulty is how to determine these stiffnesses. We have used a method described by Jolicoeur and Cardou [15]. This leads to a logical inconsistency: one of the Young's moduli, E_T, was calculated from a knowledge of the contact forces between individual wires within the rope, and these forces were estimated using Costello's theory ([4]); the inconsistency is that the latter theory gives Eq. (1) for F whereas we obtain Eq. (25) (wherein

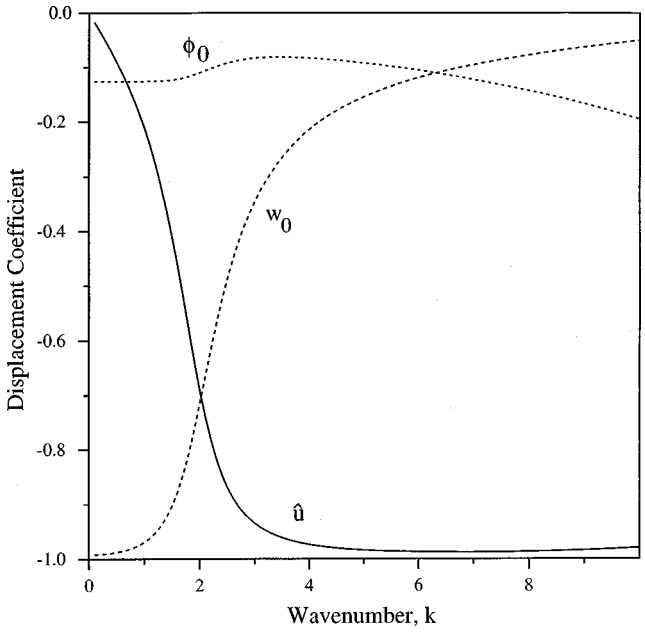

Fig. 3 The components of the dimensionless eigenvector $\mathbf{x}_2$ corresponding to the dimensionless wave speed α_2.

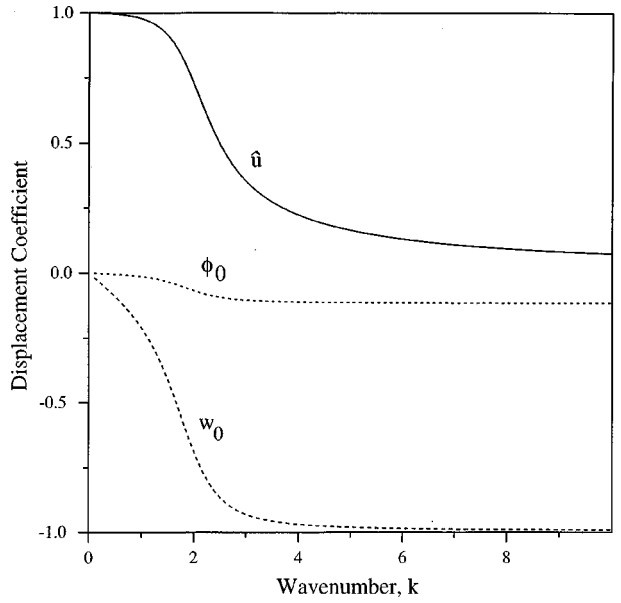

Fig. 4 The components of the dimensionless eigenvector x_3 corresponding to the dimensionless wave speed α_3.

$A_5=0$). In fact, we applied a static tension, determined the contact forces, and then superimposed a wave motion. In the absence of a better algorithm, we feel that the present approach is adequate; we note that the modulus E_T depends weakly on the actual magnitude of the contact forces, so that a rough estimate should suffice.

One aspect not considered here is that of *damping*: experimentally, it is observed that wave amplitude decays with distance along the wire rope. The precise cause of this phenomenon is unknown. For a wire rope under static tension F, it is known that interwire slippage is not responsible ([28]), although the damping does vary with F and with the number of wires comprising the rope; see [29] for a review. Further work is needed so as to develop a predictive model for damping.

Acknowledgments

This work was partially supported by the Center for Advanced Control of Energy and Power Systems, a National Science Foundation Industry/University Cooperative Research Center, at the Colorado School of Mines. We are grateful for many discussions with the Center's Director, Rahmat Shoureshi, and with other colleagues and students. We have also benefited from comments and reprints from A. Cardou and M. Raoof.

Appendix A

Rotated Stiffnesses. A material with cylindrical orthotropy has elastic stiffnesses $C'_{\alpha\gamma}$ when referred to principal axes. Rotation about the radial axis by an angle β leads to stiffnesses $C_{\alpha\gamma}$, defined as follows:

$$C_{11}=C'_{11},\quad C_{12}=C'_{12}\cos^2\beta+C'_{13}\sin^2\beta,$$

$$C_{13}=C'_{13}\cos^2\beta+C'_{12}\sin^2\beta,$$

$$C_{14}=\frac{1}{2}(C'_{13}-C'_{12})\sin 2\beta,\quad C_{22}=C'_{22}\cos^4\beta+\frac{1}{2}C'_{23}\sin^2 2\beta,$$

$$C_{23}=C'_{23}(\cos^4\beta+\sin^4\beta)+\left(\frac{1}{4}C'_{22}+\frac{1}{4}C'_{33}-C'_{44}\right)\sin^2 2\beta,$$

$$C_{24}=\frac{1}{2}(C'_{44}+C'_{23})\sin 4\beta+\frac{1}{2}(C'_{33}\sin^2\beta-C'_{22}\cos^2\beta)\sin 2\beta,$$

$$C_{33}=C'_{33}\cos^4\beta+C'_{22}\sin^4\beta+\left(C'_{44}+\frac{1}{2}C'_{23}\right)\sin^2 2\beta,$$

$$C_{34}=\frac{1}{2}(C'_{33}\cos^2\beta-C'_{22}\sin^2\beta)\sin 2\beta-\frac{1}{2}\left(C'_{44}+\frac{1}{2}C'_{23}\right)\sin 4\beta,$$

$$C_{44}=C'_{44}\cos^2 2\beta+\frac{1}{4}(C'_{33}+C'_{22}-2C'_{23})\sin^2 2\beta,$$

$$C_{55}=C'_{55}\cos^2\beta+C'_{66}\sin^2\beta,$$

$$C_{56}=\frac{1}{2}(C'_{55}-C'_{66})\sin 2\beta\ \text{ and }\ C_{66}=C'_{66}\cos^2\beta+C'_{55}\sin^2\beta.$$

Appendix B

Contact Stresses. In order to calculate E_T, we have to calculate the contact stresses between the aluminum wires and the steel core. Specifically, we require X_c, the contact force per unit length acting along the line of contact. Thus, we apply a static load to the wire rope; the axial force F, axial twisting moment M, axial strain ε, and rotation per unit length χ are related by Eq. (1). The theory in [4] yields expressions for A_1-A_4, and also for X, the contact force per unit length along the centerline of the rope. Then, X_c is given by [4], Eqs. (3.10) and (3.114), as

$$X_c=-X\{\cos^2\beta+(r_s/h)^2\sin^2\beta\}^{-1/2}=-1.011X, \qquad (B1)$$

using $\beta=10$ deg and $r_s/h=0.503$ for our ACSR conductor.

The total axial force acting on the wire rope is $F=F_0+F_1$, where F_0 and F_1 are the axial forces in the steel core and aluminum wires, respectively. We have $F_0=\pi E_s r_s^2\varepsilon$. For F_1 and X, we have the following equations from [4], Section 3.9:

$$F_1=6(T\cos\beta+N\sin\beta),$$

$$hX=(N\cos\beta-T\sin\beta)\sin\beta,$$

$$hN=(H\sin\beta-G\cos\beta)\sin\beta,$$

$$hG=\frac{1}{4}\pi E_a r_a^4(\Lambda\sin^2\beta-\alpha_1\sin 2\beta),$$

$$hH=\frac{1}{4}\pi(1+\nu_a)^{-1}E_a r_a^4(\Lambda\sin\beta\cos\beta-\alpha_1\cos 2\beta),$$

with $T=\pi E_a r_a^2\xi_1$ and $h\Lambda=\nu_s r_s\varepsilon+\nu_a r_a\xi_1$. We also have

$$\xi_1+\alpha_1\tan\beta=\varepsilon, \qquad (B2)$$

$$\xi_1\tan\beta-\alpha_1+\Lambda\tan\beta=h\chi. \qquad (B3)$$

Comparing our notation with that used in [4], we have $F_1=F_2$, $G=G'_2$, $H=H'_2$, $N=N'_2$, $T=T'_2$, $X=X_2$, $\alpha_1=\Delta\alpha_2$, $r_a=R_2$, $r_s=R_1$, $\beta=(1/2)\pi-\alpha_2$, $h=r_2$, $\chi=\tau_s$ and $\xi_1=\xi_2$. Also, $m_2=6$.

We can solve Eqs. $(B2)$ and $(B3)$ for ξ_1 and α_1:

$$\xi_1=\Omega^{-1}\{\varepsilon(h\cos^2\beta-\nu_s r_s\sin^2\beta)+\chi h^2\sin\beta\cos\beta\},$$

$$\alpha_1=\Omega^{-1}\{\varepsilon(h+\nu_s r_s+\nu_a r_a)\sin\beta\cos\beta-\chi h^2\cos^2\beta\},$$

where $\Omega=h+\nu_a r_a\sin^2\beta$. We can then substitute back, so as to obtain an expression for F in terms of ε and χ.

Let us suppose that the wire rope is subject to a prescribed static load F and that the moment M is adjusted so that the rope does not rotate ($\chi=0$). Then, we find that

$$T=\pi E_a r_a^2\varepsilon\Omega^{-1}(h\cos^2\beta-\nu_s r_s\sin^2\beta),$$

$$hG=\frac{1}{4}\pi E_a r_a^4\varepsilon\Omega^{-1}\{\nu_s r_s-(2h+2\nu_s r_s+\nu_a r_a)\cos^2\beta\}\sin^2\beta,$$

$$hH=\frac{1}{4}\pi(1+\nu_a)^{-1}E_a r_a^4\varepsilon\Omega^{-1}\{(2h+2\nu_s r_s+\nu_a r_a)\sin^2\beta - h\}\sin\beta\cos\beta.$$

If we take $\nu_s=0.25$ and $\nu_a=0.33$, we find that

$$G=-0.0259E_a r_a^3\varepsilon, \quad H=-0.0462E_a r_a^3\varepsilon,$$

$$T=3.019E_a r_a^2\varepsilon \text{ and } N=0.00151E_a r_a^2\varepsilon.$$

We can take $E_s=3E_a$, whence

$$F_0=1.07E_a a^2\varepsilon \text{ and } F_1=1.96E_a a^2\varepsilon, \tag{B4}$$

and so $F=3.03\,E_a a^2\varepsilon$. Thus, given the static load F, this equation determines the axial strain ε, whence

$$N=(5.5\times10^{-5})F, \quad T=0.11F \text{ and } hX=-0.0033F. \tag{B5}$$

Finally, we deduce from Eq. $(B1)$ that

$$hX_c=0.0033F. \tag{B6}$$

The fact that N is much smaller than T suggests that asymptotic approximations valid for small β should be useful. With errors of $O(\beta^2)$ as $\beta\to0$, we easily obtain $\Omega=h$, $\xi_1=\varepsilon$, $T=\pi E_a r_a^2\varepsilon$, $G=O(\beta^2)$, $H=O(\beta)$, $N=O(\beta^3)$,

$$F_1/(E_a a^2\varepsilon)=6\pi(r_a/a)^2=2.07$$

(which should be compared with the ''exact'' result Eq. $(B4)$) and

$$hX\sim-\pi\beta^2 r_a^2 E_a\varepsilon\sim-0.0032F,$$

using $\beta=0.17$. This result for X is in error by about 3%.

References

[1] Rawlins, C. B., 1979, ''Fatigue of Overhead Conductors,'' *Transmission Line Reference Book: Wind-Induced Conductor Motion*, Electric Power Research Institute, Palo Alto, CA, pp. 51–81.

[2] Berger, J. R., Martin, P. A., and McCaffery, S. J., 2000, ''Time-Harmonic Torsional Waves in a Composite Cylinder With an Imperfect Interface,'' J. Acoust. Soc. Am., **107**, pp. 1161–1167.

[3] Butson, G. J., Phillips, J. W., and Costello, G. A., 1980, ''Stresses in Wire Rope due to Dynamic Loads Associated With Deep Shaft Hoisting Systems,'' *Proc. First Annual Wire Rope Symposium*, Denver, CO, Engineering Extension Service, Washington State University, Pullman, WA, pp. 243–273.

[4] Costello, G. A., 1997, *Theory of Wire Rope*, 2nd Ed., Springer, New York.

[5] McConnell, K. G., and Zemke, W. P., 1982, ''A Model to Predict the Coupled Axial Torsion Properties of ACSR Electrical Conductors,'' Exp. Mech., **22**, pp. 237–244.

[6] Lanteigne, J., 1985, ''Theoretical Estimation of the Response of Helically Armored Cables to Tension, Torsion, and Bending,'' ASME J. Appl. Mech., **52**, pp. 423–432.

[7] Sathikh, S., Rajasekaran, S., Jayakumar, and Jebaraj, C., 2000, ''General Thin Rod Model for Preslip Bending Response of Strand,'' J. Eng. Mech., **126**, pp. 132–139.

[8] Raoof, M., and Kraincanic, I., 1994, ''Critical Examination of Various Approaches Used for Analysing Helical Cables,'' J. Strain Anal., **29**, pp. 43–55.

[9] Samras, R. K., Skop, R. A., and Milburn, D. A., 1974, ''An Analysis of Coupled Extensional-Torsional Oscillations in Wire Rope,'' J. Eng. Ind., **96**, pp. 1130–1135.

[10] Graff, K. F., 1991, *Wave Motion in Elastic Solids*, Dover, New York.

[11] Cardou, A., and Jolicoeur, C., 1997, ''Mechanical Models of Helical Strands,'' Appl. Mech. Rev., **50**, pp. 1–14.

[12] Hobbs, R. E., and Raoof, M., 1982, ''Interwire Slippage and Fatigue Prediction in Stranded Cables for TLP Tethers,'' *Proceedings, 3rd Intl. Conf. Behavior of Offshore Structures*, Hemisphere, Washington, DC, pp. 77–92.

[13] Blouin, F., and Cardou, A., 1989, ''A Study of Helically Reinforced Cylinders Under Axially Symmetric Loads and Application to Strand Mathematical Modelling,'' Int. J. Solids Struct., **25**, pp. 189–200.

[14] Jolicoeur, C., and Cardou, A., 1994, ''Analytical Solution for Bending of Coaxial Orthotropic Cylinders,'' J. Eng. Mech., **120**, pp. 2556–2574.

[15] Jolicoeur, C., and Cardou, A., 1996, ''Semicontinuous Mathematical Model for Bending of Multilayered Wire Strands,'' J. Eng. Mech., **122**, pp. 643–650.

[16] Skop, R. A., and Samras, R. K., 1975, ''Effects of Coupled Extensional-Torsional Oscillations in Wire Rope During Ocean Salvage and Construction Operations,'' J. Eng. Ind., **97**, pp. 485–492.

[17] Phillips, J. W., and Costello, G. A., 1977, ''Axial Impact of Twisted Wire Cables,'' ASME J. Appl. Mech., **44**, pp. 127–131.

[18] Raoof, M., Huang, Y. P., and Pithia, K. D., 1994, ''Response of Axially Preloaded Spiral Strands to Impact Loading,'' Comput. Struct., **51**, pp. 125–135.

[19] Martin, P. A., 1992, ''Boundary Integral Equations for the Scattering of Elastic Waves by Elastic Inclusions With Thin Interface Layers,'' J. Nondestruct. Eval., **11**, pp. 167–174.

[20] Ting, T. C. T., 1996, ''Pressuring, Shearing, Torsion and Extension of a Circular Tube or Bar of Cylindrically Anisotropic Material,'' Proc. R. Soc. London, Ser. A, **452**, pp. 2397–2421.

[21] Martin, P. A., and Berger, J. R., 2001, ''Waves in Wood: Free Vibrations of a Wooden Pole,'' J. Mech. Phys. Solids, **49**, pp. 1155–1178.

[22] Ting, T. C. T., 1996, *Anisotropic Elasticity*, Oxford University Press, Oxford, UK.

[23] Jones, R. M., 1999, *Mechanics of Composite Materials*, 2nd Ed., Taylor & Francis, Philadelphia, PA.

[24] Doocy, E. S., and Hard, A. R., 1979, ''Introduction,'' *Transmission Line Reference Book: Wind-Induced Conductor Motion*, Electric Power Research Institute, Palo Alto, CA, pp. 1–50.

[25] Young, W. C., 1989, *Roark's Formulas for Stress and Strain*, 6th Ed., McGraw-Hill, New York.

[26] Abramowitz, M., and Stegun, I. A., eds., 1965, *Handbook of Mathematical Functions*, Dover, New York.

[27] Boström, A., 2000, ''On Wave Equations for Elastic Rods,'' Z. Angew. Math. Mech., **80**, pp. 245–251.

[28] Labrosse, M., Nawrocki, A., and Conway, T., 2000, ''Frictional Dissipation in Axially Loaded Simple Straight Strands,'' J. Eng. Mech., **126**, pp. 641–646.

[29] Fang, J., and Lyons, G. J., 1996, ''Structural Damping of Tensioned Pipes With Reference to Cables,'' J. Sound Vib., **193**, pp. 891–907.